RECONSTRUCTION OF FULL FIBER ORIENTATION DISTRIBUTION IN MOLDED COMPOSITES USING DEEP LEARNING

Mohammad Nazmus Saquib[1], Siavash Sattar[1], Richard Larson[1], Jiang Li[1], Sergii G. Kravchenko[2], Oleksandr G. Kravchenko[1]

[1]Old Dominion University, Department of Mechanical Aerospace Engineering, Norfolk, Virginia

[2]Department of Materials Engineering, University of British Columbia, Vancouver, BC, Canada

Abstract

Molded composite materials are key to the functionality, mobility, and sustainability of electric vehicles (EVs), on-demand air mobility, and aerospace structures. Fiber orientation distribution (FOD) characterization of composite materials is necessary to understand the mechanical variability in prepreg platelet molded compounds (PPMC). A novel U-Net deep learning model was developed to predict the local through-thickness fiber orientation (FOD) field in PPMC composites using the thermal strain field as an input. The deep learning model was trained with synthetically generated PPMC morphologies and tested on a molded plaque. Thousands of virtual PPMC plates were subjected to uniform temperature change and used to collect the thermal strain components (ϵ_{xx}, ϵ_{yy}, ϵ_{xy}) on the surface of PPMC plates. The strain components were used to train the U-Net model to predict average through-thickness FOD in the entirety of the molded plate. A heating stage with a digital image correlation (DIC) setup was developed to analyze the thermal expansion behavior of PPMC samples. The trained deep learning U-Net model was used to predict FOD in a physical part by providing surface strain fields collected through thermal DIC. The obtained U-Net model prediction of FOD was compared to FOD obtained through microscopy and image analysis. The predicted non-uniform behavior of FOD was compared with the experimentally measured FOD along several polished cross-sections and revealed close agreement. The present results indicate the opportunity for rapid inspection to detect manufacturing-induced FOD in molded composites using the proposed deep learning model.

Introduction

Prepreg-Platelet Molded Composites (PPMC) are an important section of the molded composites, as it has better processability into complex geometric shapes to be used in the automotive and aerospace industry [1], [2]. PPMCs are discontinuous fiber reinforced polymer composites made from slitting prepreg tapes heat pressed within a mold to give desired form [3]. PPMCs offer high structural grade properties although made with discontinuous fibers [4]–[10]. FOD in a PPMC depends on several factors including material deposition, compaction, flow direction, heat supplied, pressure applied, etc. [11]. Due to high material anisotropy, PPMC exhibits complex mechanical behaviors as platelets during production could not be deposited in a controlled way [12]. Hence, PPMC's FOD is locally varying from production due to stochastic deposition during manufacturing. Variations of FODs locally in PPMC morphology are known as manufacturing-induced signatures. Spatial variability of FOD leads to the local variation of thermo-mechanical properties of the PPMC throughout the plate. Although many industrial-scale productions have the same global orientation, variations of FOD locally make each part unique [8]. After the application of uniform temperature differential, varying deformation configuration on the surface of the PPMC was found due to local FOD variation on the PPMC plaque [13].

To know the physical-mechanical properties of composite material, it is important to find its fiber orientation [14]. Conventional Non-destructive evaluation (NDE) methods like flash-

tomography and pulse echo C-scan ultrasound can detect voids, and defects but these are currently unable to analyze local FOD in PPMC [15]. Some traditional FOD inspection methods like optical microscopy and micro-computed tomography (μCT) are proven to deliver accurate analysis, but they are time-consuming [16], [17]. Some other limitations include the destructive nature of the optical microscopy process and μCT having a restriction on analyzing larger specimens [18]. A reliable rapid inspection method for characterizing the FOD of PPMC mesostructures is a necessity for predicting structural mechanical properties to ensure composite reliability.

Data-driven modeling is becoming popular day by day. The application of Artificial Intelligence (AI) and Machine Learning (ML) was found useful to solve many composite manufacturing and performance-related problems [19]. Application of deep learning extracts and analyses information from images using machine learning techniques [18]. Image classification and semantic segmentation in deep learning enable to store fine detailed information about an object. For quality inspection at different stages of manufacturing and to predict FOD within, computer vision should be considered [21], [22]. In this study, a new method was proposed to combine thermal DIC response and artificial neural network rapid FOD analysis.

A fully convolutional network (FCN) U-Net, which is a pixel-based image segmentation model, was used throughout our work to predict the manufacturing-induced FOD in PPMC plates. Fiber orientations on the PPMC averaged through the thickness were predicted based on the images of the full field strain distribution on the PPMC plates. Experimental images of strain distributions were captured via the thermal DIC technique on the top and bottom surface of the PPMC plate and applied to the trained U-Net model to predict FOD. This paper describes the proposed method, accuracy, and validity of the developed U-Net model for predicting local FOD. Thermal DIC strain data was used to provide the input of the algorithm to predict FODs in a PPMC plate, whereas optical microscopy image analysis was used to measure and validate the predicted FOD on the surface of the PPMC plates [17], [23], [24].

Method

The proposed framework uses virtual PPMC morphology for extracting the calculated data obtained via linear finite element analysis. Next, U-Net model training is conducted along with model performance evaluation using experimental validation. U-Net is a type of FCN, which is different from the regular contracting convolutional neural network (CNN). U-Net allows for up-sampling expansion that provides the same resolution of the predicted output data (FOD field), as the input resolution (strain fields). Specifically, average through-thickness FOD was predicted by U-Net from a given strain field. U-Net was also used because it can work with fewer training images to provide better segmentation in a comparatively lesser amount of time [25].

The structure of the reconstruction of FOD and its prediction in PPMC plate is shown in Figure 1. A finite element model was developed to simulate PPMC response under uniform thermal loading. Ten thousand of virtual morphologies and corresponding strain data were used to train the U-Net model. The advantage of using the high-fidelity synthetic morphology is apparent when considering the amount of time that would be required to generate the equivalent number of experimentally molded samples, followed by the FOD evaluation for ML training and thermal expansion experiments. The use of the synthetic data is also free from the associated experimental errors during all of the specified steps. Upon completion of training, U-Net can rapidly predict local through-thickness FOD in PPMC. To experimentally validate U-Net performance, experimental strain data obtained from thermal DIC was used as input for the trained U-Net model to predict the through-thickness FOD of the respective sample. The FOD prediction was compared with the measurement of FOD via microscopic analysis using image

segmentation.

The reconstruction of the FOD study is mainly comprised of two parts: a) A forward linear finite element model to extract strain data on the part surface due to the uniform temperature change of PPMC plates, b)To solve the inverse problem utilizing strain data from finite element analysis output to predict FOD in a PPMC plate. The second part is solved using FCN. The FCN was trained to form a relation between strain fields and FOD identifying parameters.

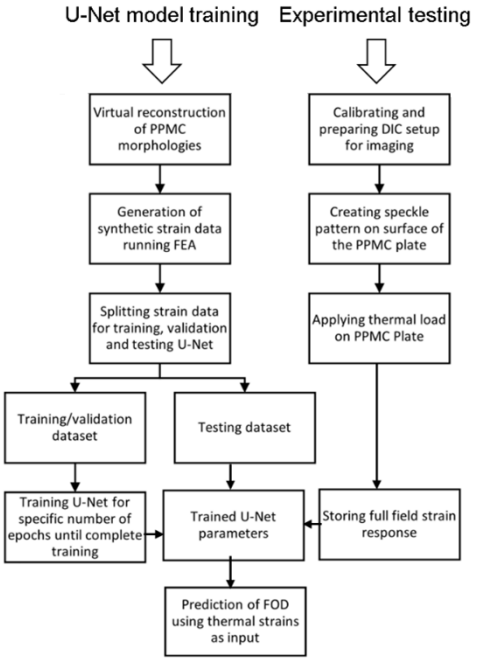

Figure 1: Framework of FOD reconstruction in PPMC using U-Net.

Generation of synthetic datasets

Virtual PPMC morphologies were modeled in Digimat FE e-Xtream Engineering defining specimen dimensions, platelet dimensions, and global fiber orientations as input. A representation of virtual PPMC morphology produced by Digimat is shown in Figure 2. The morphologies were then imported into ABAQUS/Standard to perform FE analysis. The platelet dimensions for PPMC were set as 6.35 x 12.7 x 0.13 mm and the PPMC plate dimensions as 126.4 x 126.4 x 1.95 mm. The prepreg tapes used for the analysis are IM7/8552. A Uniform temperature difference was applied to the PPMC plate to perform the thermo-elastic analysis. The full PPMC plate was then meshed into 160 x 160 x 15 eight brick node C3D8 finite element voxels, each having dimensions 0.79 x 0.79 x 0.13 mm for performing the FE analysis.

PPMC structures with the same global FOD typically had different locally variable FOD due to the Monte Carlo method of generating the synthetic PPMC morphologies. Application of uniform thermal load on PPMC plates results in non-uniform strain responses throughout the surface. These strain fields ($\epsilon_{xx}, \epsilon_{yy}, \epsilon_{xy}$) were provided as input to U-Net later to predict locally varying FOD in PPMC morphologies.

A python script was generated to produce multiple PPMC morphologies with different global orientations (A_{xx}= 0.1, 0.3, 0.5, 0.7, 0.9), and FOD varying locally within the plates. A_{xx} is the probability of finding fiber alignment in an X-direction. Another script was used to import these

morphologies in ABAQUS and perform FE analysis to extract surface strain fields on the top and bottom surfaces of the PPMC plates. The results were stored as arrays of structured data and used in U-Net training later.

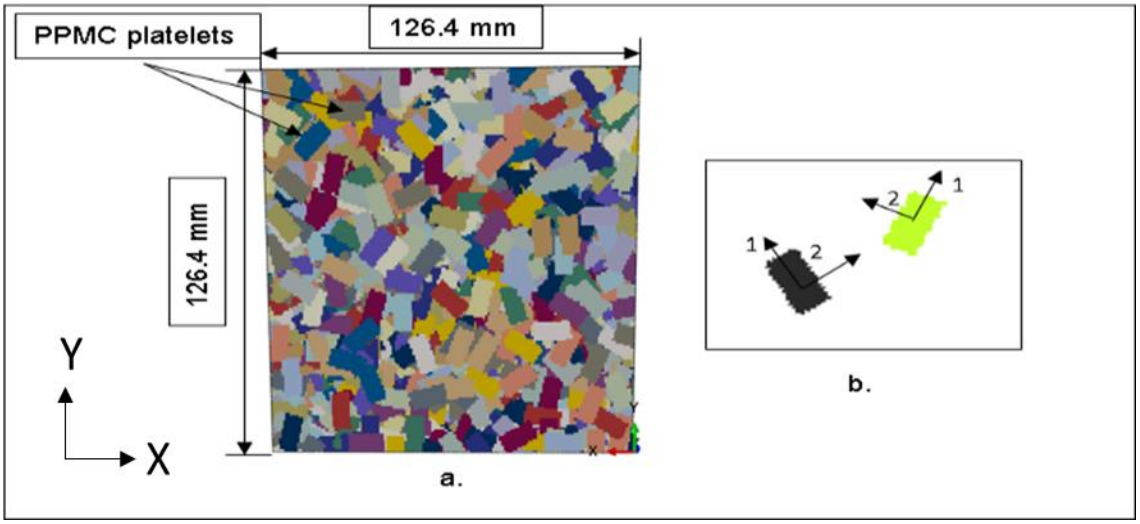

Figure 2: a) Digital PPMC morphology with locally varying FOD; b) Individual PPMC platelets in space.

The PPMC plate was constructed with 160 elements on both the X and Y-axis. It was treated as a 160 x 160-pixel image to be used for Fully Convolutional Network (FCN). From the FE analysis, local FOD characteristics (A_{11}, A_{12}) and surface strains ($\epsilon_{xx}, \epsilon_{yy}, \epsilon_{xy}$) of top and bottom surfaces were stored.

Deep Learning Model for FOD reconstruction

The input for U-Net training was the structured data array of surface strains, which were obtained from FE analysis. The surface strain data of the PPMC plate was stored as a 160 x 160 x 6 data array. The 160 x 160 data points were strain data of each element voxels and the 6 depth channels were surface strains ($\epsilon_{xx}, \epsilon_{yy}, \epsilon_{xy}$) of top and bottom surfaces. The U-Net training was done using 25 patches with 32 x 32 x 6 voxel dimensions. Thus, the extracted patches covered the whole in-plane 160 x 160 voxels of the synthetic PPMC plate. The total number of patches used for training, testing, and validation was 2,50,000 with 70,15,15% split, respectively. The neurons (weights and biases) of the neural network were arranged as layers to give an output, whereas filters help to extract unique features in the sample. 4 such U-Net layers and 128 filters were used for its training purpose. The U-Net trained with data extracted from total 10,000 morphologies having global FOD, A_{xx} = 0.1, 0.3, 0.5, 0.7, 0.9. For each global FOD state, equal 2000 morphologies were generated for training purposes. An epoch is the complete travel of the training dataset through the algorithm. 4000 such epochs were performed to complete the training process.

Digital Image Correlation and extraction of thermal strain fields

Digital Image Correlation (DIC) is a non-contact process that compares different images of a specimen at different deformation stages due to applied load, taken at a time interval. The system tracks pixel displacement with respect to the reference undeformed configuration of the image to calculate the strain field components. The experimental setup for this study consisted of two cameras, a heating chamber, a temperature controller, external light sources, and a computer

with GOM Snap software. The schematic of the overall experimental setup is shown in Figure 3. The two cameras capture timed pictures during the heating cycle. The heating chamber used thermal insulation to ensure the application of uniform thermal load on the PPMC surface. Quartz glass was used to cover the heating chamber, as it helps to keep the heating stage insulated. The PPMC specimen was also placed upon a hollow square to ensure a uniform heat load was applied to it.

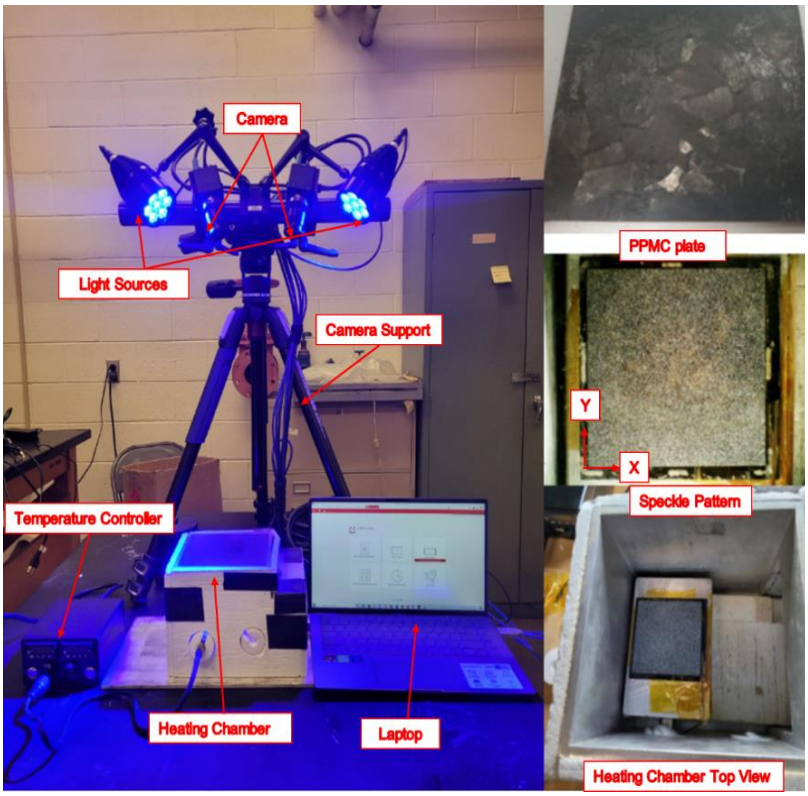

Figure 3: Schematic of Digital Image Correlation Experimental Setup.

Before starting the process, the PPMC plate was painted to create speckle patterns on both, top and bottom surfaces, to analyze deformation during a thermal expansion (Figure 3). The temperature inside the heating chamber was elevated from room temperature with the help of a temperature controller to create a temperature difference. The painted specimen was placed inside the insulated heating chamber to minimize any kind of heat loss as much as possible. The sample was then heated following a ramp of 1.3°C/min. To apply thermal load uniformly, isothermal heat was applied for 45 minutes, followed by the cooldown stage. During the application of load, an image was taken each minute and stored. The heating cycle was recorded by the thermo-couple inside the heating chamber and is shown in Figure 4. Two sets of images were captured for calculating the deformation of the specimen once the thermal equilibrium was reached during the iso-thermal stage: strain data was recorded at Time-1 (136 minutes), and Time-2 (166 minutes). Time 1 was selected after reaching the isotherm and Time 2 was 30 minutes into the isothermal stage. The same steps were repeated for the other surface (top/bottom) to capture specimen deformation images.

All the images captured were imported into GOM Correlate to extract deformation data. Firstly, surface strain components were created on the PPMC specimen (63.5 x 63.5 x 1.95 mm) reference image using the squared facets metric. Squared facets were set at 19 pixels and a point

distance of 16 pixels. These squared facets identify painted stochastic patterns within its space and later track the change of its position gradually with the application of load to find deformation. 81 x 81 such data points were created on the surface of the PPMC specimen to extract full-field strain distribution (ϵ_x, ϵ_y, ϵ_{xy}). MATLAB griddata function for 2-D data interpolation using nearest method for discontinuous data interpolation was used to sort the extracted strain fields to specific grid locations, determined by the pixel size in U-Net training to get full field FOD as output. 0.79 x 0.79 mm grid sizes were maintained to match the finite element mesh sizes, which were used to generate the synthetic datasets to be used for U-Net training. Strain data were extracted, sorted and stored this way using image sets captured at Time 1 and Time 2. Strain field at two different times during isothermal heating stage were averaged before using as U-Net input. Strain distributions of both front and back of the specimen were provided as an input and passed through the trained U-Net 4 layers and 128 filters of weights and biases to predict the average through-thickness FOD of the specimen.

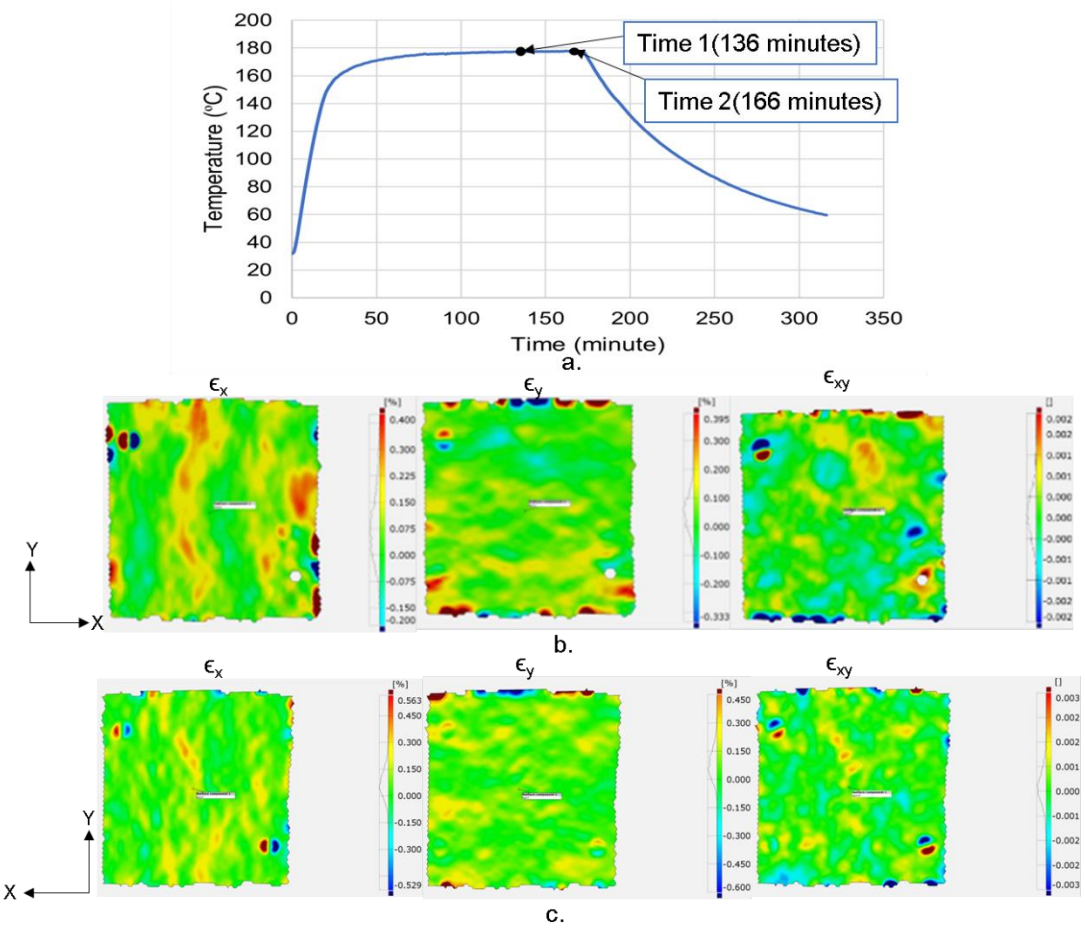

Figure 4: a) Full-field application of thermal load inside the heating chamber; b) Thermal strains (ϵ_x, ϵ_y, ϵ_{xy}) heatmap on the front surface of PPMC plate; c) Thermal strains (ϵ_x, ϵ_y, ϵ_{xy}) heatmap on back surface of the PPMC plate

Optical microscopy and image analysis to characterize FOD

Optical microscopy and image analysis combination were used to characterize FOD locally through the thickness. A 63.5 x 63.5 mm sample PPMC plate was used for inspection. The plate was cut open along 14.5-mm and 31.75-mm lines from the top for inspecting and measuring local FOD. The cut-through samples were mounted for microscopy using epoxy resin and then went through seven stage polishing process: 300, 400, 600, 800, and 1200 grit sandpaper grinding, followed by 3 µm and 1 µm deagglomerated diamond polishing. The prepared sample was then taken to a Leica DM6 M microscope for microscopic analysis. The micrographs were captured in 38 different segments, 1.67 x 1.95 mm each, and stitched together using Leica software. Microscope-captured greyscale images are shown in Figure 5a.

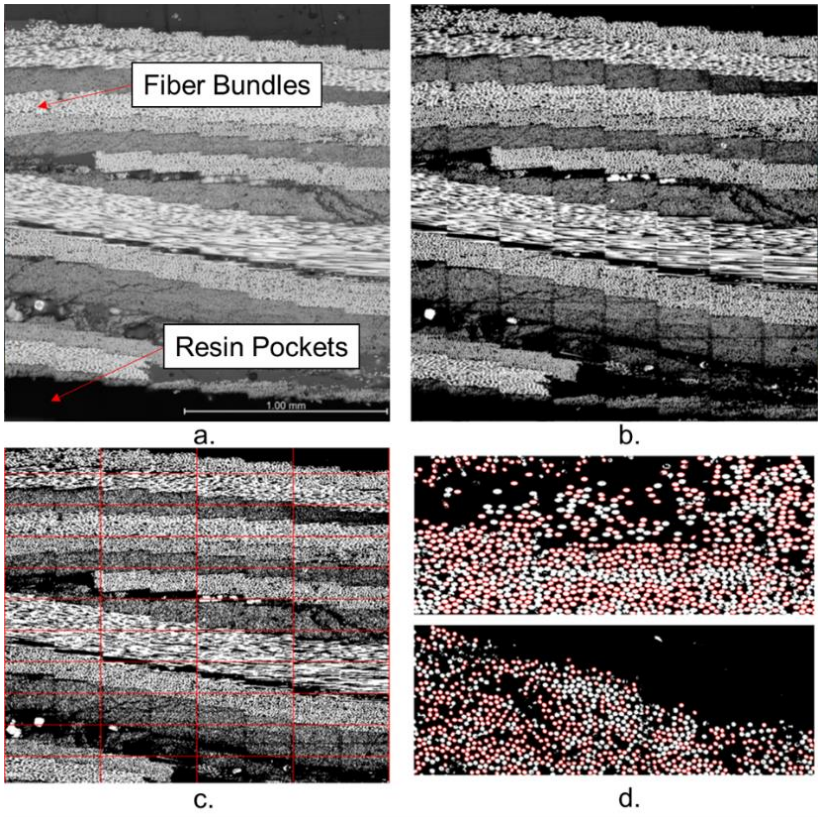

Figure 5: a) 8-bit greyscale micrograph of 1/38th part of the PPMC plate along the length; b) binarized, filtered and segmented 2-bit micrograph; c) 4 x 12 grid line segmentation of the micrograph for accurate measurements; d) Ellipse measurement within a grid using MATLAB image processing toolbox to characterize FOD.

The 8-bit grayscale micrographs captured were taken into ImageJ software to binarize, filter, and segment them (Figure 5b). After complete binarization, the black and white colors in the micrograph referred to the matrix and fibers in the PPMC plate. The threshold of the binarization was adjusted in such a way that, the micrograph can represent the fiber boundaries accurately. The binarized image was then taken into MATLAB for FOD measurement with the help of the image processing toolbox. First, the micrographs were segmented into 4 x 12 grids, and then the image was split into 48 parts according to the grids (Figure 5c). It was split in such a way to find similar fibers within the image, which helps the MATLAB script to identify and fit ellipses perfectly for FOD measurements. The grid segmentation representation of the micrograph is shown in Figure 5d. Some of the fiber bundles contain almost parallel to the plane long fibers, which are

very difficult to capture by MATLAB image processing. Those segmented micrographs were taken into Ellipse fit software to measure and calculate the fiber orientation manually. Some of the images were also analyzed using EllipseFit to cross-check and validate MATLAB image processing.

Results

Virtual testing of U-Net Response

15% of synthetic datasets produced were stored for testing purposes. A method of testing U-Net response virtually is to pass a randomly selected PPMC plate through U-Net for FOD prediction and compare it with the ground truth value. Figure 6 shows the heatmap comparison of the U-Net prediction of spatial FOD of a PPMC plate with its actual FOD. The region with a darker shade exhibits a higher degree of fiber alignment region in the X-direction. One difference is the prediction seems to show less sharpness in some places of higher alignment. Other than that, it can be conferred that model is correctly predicting local FOD for the virtual responses.

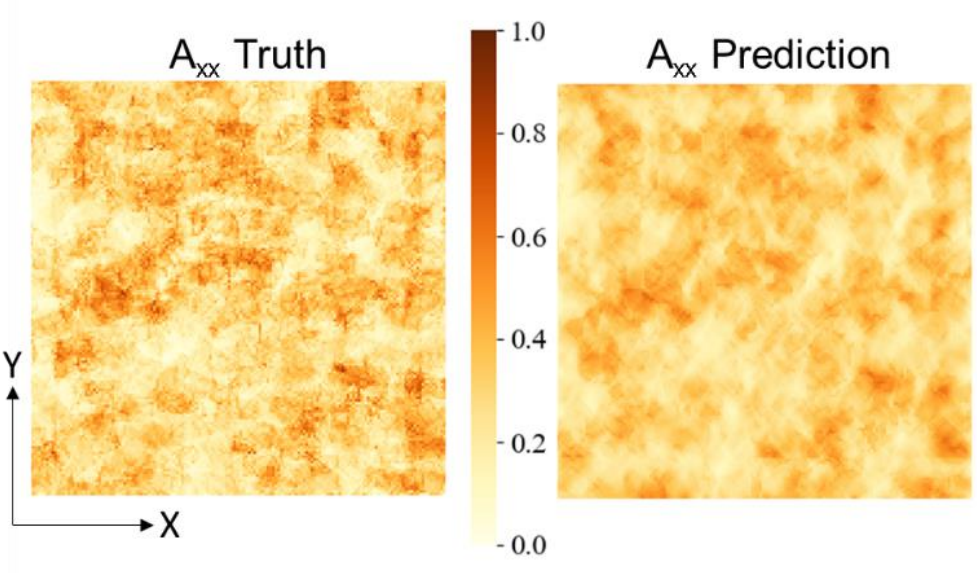

Figure 6: Truth vs Prediction heatmap of a random plate tested on U-Net.

Comparison of FOD measurement with U-Net prediction

The FOD measurement of each grid was averaged column-wise to get a local average degree of alignment along the X-axis through the thickness. Image representation of voxelized FOD calculation is shown in Figure 7. All fibers aligned almost parallel to the X-axis were found to have A_{xx} close to 1 and fibers perpendicular to X-axis were measured close to 0. Again, fibers with a smaller elliptical cross-section having close minor and major diameter values were measured to have significantly higher A_{xx} compared to fibers with a bigger elliptical cross-section having a minor diameter significantly smaller than its major diameter.

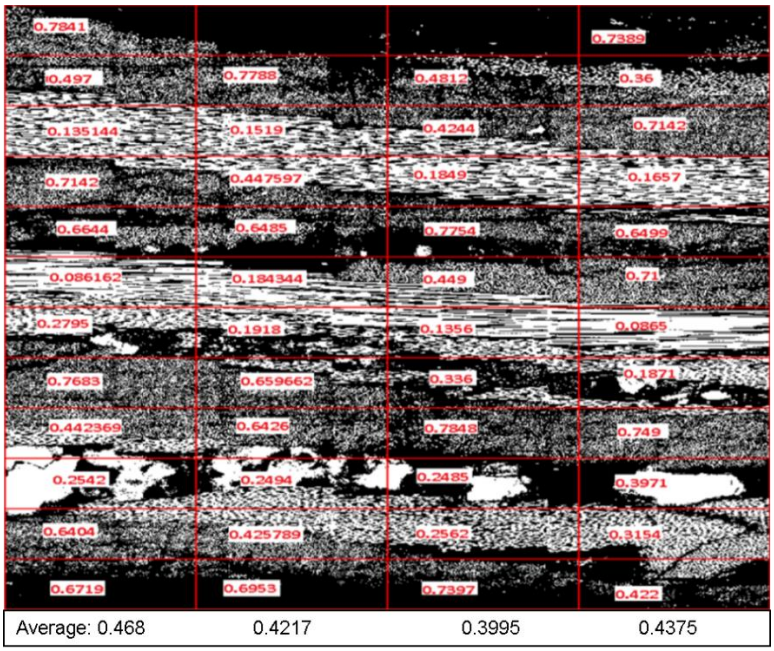

Figure 7: Measurement of A_{xx} in individual platelets to get average FOD through thickness locally.

PPMC plate FOD distribution was measured along 14.5mm and 31.75mm lines from the top edge of the surface. 14.5 mm line was symbolized as line 1 and 31.75mm line as line 2. Line 1 showed a lower degree of alignment in FOD along X-axis compared to line 2. The presence of long and larger elliptical fibers along the X-axis resulted in lower A_{xx} values. Resin-rich pocket regions are also responsible for variability in FOD. FOD measurement along line 1 and line 2 is shown in Figure 8 below.

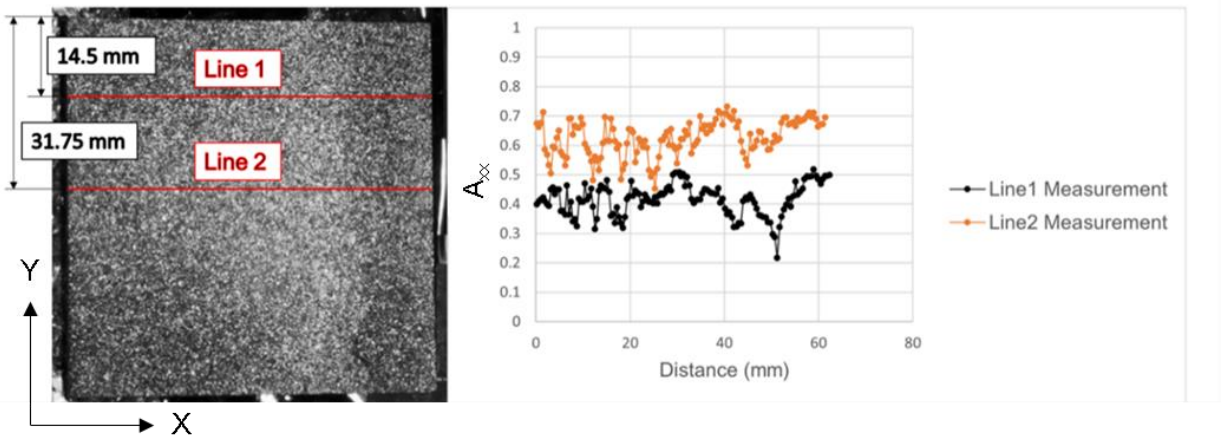

Figure 8: Measurement of FOD along line 1 and line 2 to check fiber orientation variation locally.

Measurement along different lines and U-Net predictions in the same place are compared in Figure 9. Line 2 was selected for comparison along the middle of specimen, whereas line 1 was selected based on the U-Net prediction, where heatmap was showing higher variability and lower value in fiber alignment along X-direction.

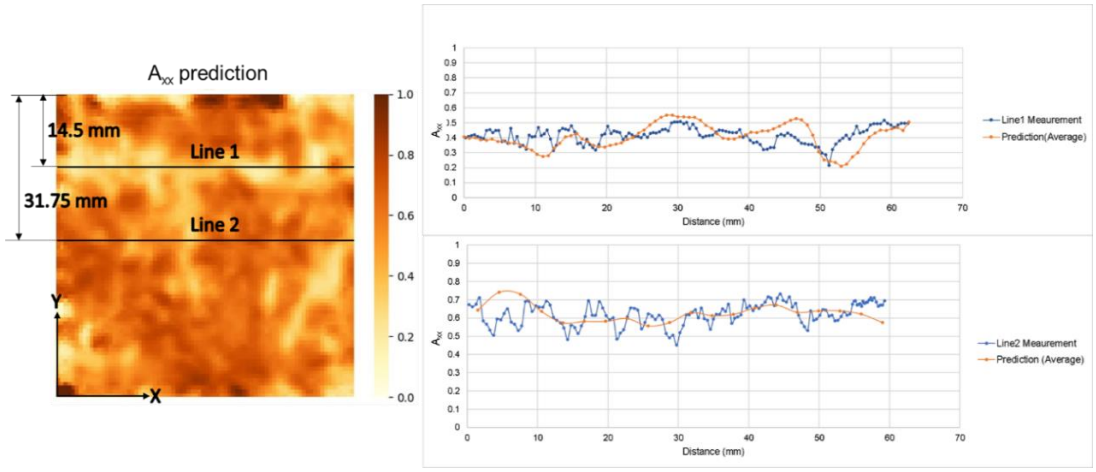

Figure 9: Measurement vs Prediction comparisons along inspection lines in a PPMC plate.

U-Net predictions were made based on the thermal DIC strain data. Strain fields were extracted on two different times during isothermal heating and were averaged to predict full field FOD via U-Net. Later, U-Net prediction was compared with measurement for validation. For Line 1, some variation in FOD was found between U-Net prediction and measurement data in the latter half of the specimen. There was a difference also in the strain data extracted during two times during isothermal heating stage. This happened due to unexpected heat loss during experiment performance. To minimize this effect, strain extracted at two different times were averaged before using as U-Net input. Other than this, the rest of the line FOD measurement revealed a close comparison with test prediction along line 1 giving 13.99% error on an average.

For Line 2, FOD measurements and prediction average showed a similar trend along the line. The U-Net prediction along line 2 gave 7.02% error in comparison with FOD measurement along same line. Measurement of FOD leads to some high peak and low peak points. Optical microscopy micrographs with even smaller dimensions to extract more data points along the line would minimize this discrepancy. It can be conferred from the line Inspection that, the U-Net model can accurately predict local FOD in a PPMC plate.

Conclusion

The developed U-Net model established a relation between supplied deformation data and spatially non-uniform through-thickness average component of fiber orientation tensor in PPMC. The partially defined inverse problem was solved by deep learning, wherein the thermal strain fields on the top and bottom surfaces of the part were used to predict local FOD in the PPMC plate. The deep learning model was trained and validated using 10000 virtual PPMC morphologies with varying degrees of fiber alignment. Based on the machine learning training and validation the model was found to predict fiber orientation with average error of 6.3%. To validate the model, a physical PPMC strain response was generated via thermal DIC setup and was used for the U-Net model. The PPMC plate was cut for polishing along the specific locations to measure FOD. Image analysis of the fiber ellipses was conducted to measure FOD through the thickness and compared with U-Net prediction. In comparison with U-Net prediction, FOD measurement revealed similarity in trend after inspections and image analysis. The functioning U-Net model allows for microstructure reconstruction and opens possibilities to rapidly inspect local variability of FOD in PPMC components allowing to capture the manufacturing-induced signature of the part.

Bibliography

[1] Tim Osswald, *Discontinuous Fiber Composites.* 2019.

[2] S. Alam and M. N. Saquib, “Impact Analysis of a Composite Armor System,” Nov. 2019. doi: 10.1115/IMECE2019-11748.

[3] S. Sattar, B. B. Laredo, D. Pedrazzoli, M. Zhang, and O. G. Kravchenko, “Understanding Size Effects on Flexural Properties in Discontinuous Fiber Reinforced Nylon Composites,” in *CAMX,* 2020, p. 15.

[4] I. Taketa, T. Okabe, H. Matsutani, and A. Kitano, “Flowability of unidirectionally arrayed chopped strands in compression molding,” *Composites Part B: Engineering*, vol. 42, no. 6, pp. 1764–1769, Sep. 2011, doi: 10.1016/j.compositesb.2011.01.021.

[5] B. Landry, A. Levy, P. Hubert, D. Leblanc, S. Roy, and A. Yousefpour, “Compression moulding of complex parts using randomly-oriented strands thermoplastic composites Thermoplastic Composites Adhesion View project Multiphysical simulation in composites forming processes View project COMPRESSION MOULDING OF COMPLEX PARTS USING RANDOMLY-ORIENTED STRANDS THERMOPLASTIC COMPOSITES,” 2014. [Online]. Available: https://www.researchgate.net/publication/263231423

[6] D. E. Sommer, S. G. Kravchenko, B. R. Denos, A. J. Favaloro, and R. B. Pipes, “Integrative analysis for prediction of process-induced, orientation-dependent tensile properties in a stochastic prepreg platelet molded composite,” *Composites Part A: Applied Science and Manufacturing*, vol. 130, Mar. 2020, doi: 10.1016/j.compositesa.2019.105759.

[7] S. G. Kravchenko *et al.*, “Tensile properties of a stochastic prepreg platelet molded composite,” *Composites Part A: Applied Science and Manufacturing*, vol. 124, Sep. 2019, doi: 10.1016/j.compositesa.2019.105507.

[8] S. G. Kravchenko, D. E. Sommer, B. R. Denos, W. B. Avery, and R. B. Pipes, “Structure-property relationship for a prepreg platelet molded composite with engineered meso-morphology,” *Composite Structures*, vol. 210, pp. 430–445, Feb. 2019, doi: 10.1016/j.compstruct.2018.11.058.

[9] S. Sattar, B. B. Laredo, D. Pedrazzoli, M. Zhang, and O. G. Kravchenko, “Understanding Size Effects on Flexural Properties - SAMPE,” in *SAMPE North America*, Sep. 2020, p. 15. Accessed: Aug. 14, 2022. [Online]. Available: https://www.nasampe.org/store/viewproduct.aspx?id=17720565

[10] S. Sattar, B. Beltran Laredo, R. Larson, S. Kravchenko, and O. G. Kravchenko, “Effect of Platelet Length and Stochastic Morphology on Flexural Behavior of Prepreg Platelet Molded Composites.”

[11] J. Teuwsen, S. K. Hohn, and T. A. Osswald, “Direct fiber simulation of a compression molded ribbed structure made of a sheet molding compound with randomly oriented carbon/epoxy prepreg strands—a comparison of predicted fiber orientations with computed tomography analyses,” *Journal of Composites Science*, vol. 4, no. 4, 2020, doi: 10.3390/jcs4040164.

[12] D. E. Sommer, S. G. Kravchenko, and R. B. Pipes, “A numerical study of the meso-structure variability in the compaction process of prepreg platelet molded composites,” *Composites Part A: Applied Science and Manufacturing*, vol. 138, Nov. 2020, doi: 10.1016/j.compositesa.2020.106010.

[13] R. Larson, R. Hoque, V. Jamora, J. Li, S. G. Kravchenko, and O. G. Kravchenko, “Prediction of Local Fiber Orientation State in Prepreg Platelet Molded Composites via Deep Convolutional Neural Network.”

[14] S. B. Visweswaraiah, M. Selezneva, L. Lessard, and P. Hubert, “Mechanical characterisation and modelling of randomly oriented strand architecture and their hybrids – A general review,” *Journal of Reinforced Plastics and Composites*, vol. 37, no. 8, pp. 548–580, Apr. 2018, doi: 10.1177/0731684418754360.

[15] P. Feraboli, T. Cleveland, M. Ciccu, P. Stickler, and L. DeOto, “Defect and damage analysis of advanced discontinuous carbon/epoxy composite materials,” *Composites Part A: Applied Science and Manufacturing*, vol. 41, no. 7, pp. 888–901, Jul. 2010, doi: 10.1016/j.compositesa.2010.03.002.

[16] P. Bing, X. Hui-min, H. Tao, and A. Asundi, “Measurement of coefficient of thermal expansion of films using digital image correlation method,” *Polymer Testing*, vol. 28, no. 1, pp. 75–83, Feb. 2009, doi: 10.1016/j.polymertesting.2008.11.004.

[17] O. G. Kravchenko, S. G. Kravchenko, A. Casares, and R. B. Pipes, “Digital image correlation measurement of resin chemical and thermal shrinkage after gelation,” *Journal of Materials Science*, vol. 50, no. 15, pp. 5244–5252, Aug. 2015, doi: 10.1007/s10853-015-9072-3.

[18] B. R. Denos, D. E. Sommer, A. J. Favaloro, R. B. Pipes, and W. B. Avery, “Fiber orientation measurement from mesoscale CT scans of prepreg platelet molded composites,” *Composites Part A: Applied Science and Manufacturing*, vol. 114, pp. 241–249, Nov. 2018, doi: 10.1016/j.compositesa.2018.08.024.

[19] H. Fernandes *et al.*, “Machine learning and infrared thermography for fiber orientation assessment on randomly-oriented strands parts,” *Sensors (Switzerland)*, vol. 18, no. 1, Jan. 2018, doi: 10.3390/s18010288.
[20] A. Garcia-Garcia, S. Orts-Escolano, S. Oprea, V. Villena-Martinez, P. Martinez-Gonzalez, and J. Garcia-Rodriguez, “A survey on deep learning techniques for image and video semantic segmentation,” *Applied Soft Computing Journal*, vol. 70. Elsevier Ltd, pp. 41–65, Sep. 01, 2018. doi: 10.1016/j.asoc.2018.05.018.
[21] T. Sabiston, K. Inal, and P. Lee-Sullivan, “Application of Artificial Neural Networks to predict fibre orientation in long fibre compression moulded composite materials,” *Composites Science and Technology*, vol. 190, Apr. 2020, doi: 10.1016/j.compscitech.2020.108034.
[22] D. M. Dimiduk, E. A. Holm, and S. R. Niezgoda, “Perspectives on the Impact of Machine Learning, Deep Learning, and Artificial Intelligence on Materials, Processes, and Structures Engineering,” *Integrating Materials and Manufacturing Innovation*, vol. 7, no. 3. Springer Science and Business Media Deutschland GmbH, pp. 157–172, Sep. 01, 2018. doi: 10.1007/s40192-018-0117-8.
[23] B. Landry and P. Hubert, “Experimental study of defect formation during processing of randomly-oriented strand carbon/PEEK composites,” *Composites Part A: Applied Science and Manufacturing*, vol. 77, pp. 301–309, Oct. 2015, doi: 10.1016/j.compositesa.2015.05.020.
[24] S. Sattar, B. Beltran Laredo, D. Pedrazzoli, M. Zhang, S. G. Kravchenko, and O. G. Kravchenko, “Mechanical behavior of long discontinuous glass fiber nylon composite produced by in-situ polymerization,” *Composites Part A: Applied Science and Manufacturing*, vol. 154, Mar. 2022, doi: 10.1016/j.compositesa.2021.106779.
[25] W. Weng and X. Zhu, “U-Net: Convolutional Networks for Biomedical Image Segmentation,” *IEEE Access*, vol. 9, pp. 16591–16603, May 2015, doi: 10.48550/arxiv.1505.04597.